Journal of Alloys and Compounds 509 (2011) 503–507

Contents lists available at ScienceDirect

Journal of Alloys and Compounds

journal homepage: www.elsevier.com/locate/jallcom

A vanadium-based conversion coating as chromate replacement for electrogalvanized steel substrates

Zhongli Zou, Ning Li*, Deyu Li, Haiping Liu, Songlin Mu

Department of Applied Chemistry, School of Chemical Engineering & Technology, Harbin Institute of Technology, Harbin 150001, PR China

ARTICLE INFO

Article history:
Received 6 April 2010
Received in revised form
16 September 2010
Accepted 17 September 2010
Available online 24 September 2010

Keywords:
Electrogalvanized steel
Vanadium
Chemical conversion coating
Corrosion resistance
X-ray techniques

ABSTRACT

The vanadium conversion coating as chromate replacement was prepared on electrogalvanized steel (EG) plates previously treated in a solution mainly composed of vanadate. Corrosion behavior of these EG plates in contact with 3.5% NaCl solution was investigated using potentio-dynamic measurement and electrochemical impedance spectroscopy (EIS) measurement. The morphology and composition of the vanadium conversion coating were studied using scanning electron microscopy (SEM) and X-ray photoelectron spectroscopy (XPS) in conjunction with argon-ion sputtering. According to the results, the V-treated EG plate shows the best corrosion protection property compared with the untreated and Cr-treated EG plates. The vanadium-rich coating is composed of the closely packed particles. The coating mainly consists of vanadium and oxygen, which mainly exist as V_2O_5, VO_2, and its hydrates such as $V_2O_5{\cdot}nH_2O$, $VO(OH)_2$.

1. Introduction

Conversion coating can improve protection for metallic surface in aggressive environment. They modify the metal surface from an active to a passive state by dipping the metal in a specific anion containing bath which reacts with the surface, forming a conversion coating. Chromating on electrogalvanzied steel, aluminum and tinplates is widely used in the automotive and aerospace industries as well as in electronics and domestic appliances [1]. However, the baths are prepared with hexavalent chromium, which is carcinogenic. Therefore, new alternative and more environmentally friendly surface treatments need to be developed [2]. Many studies have been conducted in recent decades to find a suitable friendly anticorrosive alternative to chromate. Several processes are based on different salt, expected to be less environmentally aggressive than the chromate, such as molybdate [3–5], permanganate [6,7], silicate [8–11], titanate [12–14], rare earth salts [15–18], tungstate [19,20] compounds.

Vanadium has not received in-depth consideration as chromate conversion coating replacement due to the solubility of crystalline vanadium oxides. There are relatively few coating chemistries in which vanadium or its compounds is the primary film-forming agent. Some papers reported the application of vanadate coatings on aluminum alloys and magnesium alloys. Hamdy et al. [21,22] studied the corrosion protection performance of thickened oxide conversion coatings containing vanadium ions formed on aluminum composites and proposed newly developed environmentally acceptable surface treatments based on vanadate prepared by sol–gel method. Guan and Buchheit [23] studied the self-healing properties of vanadate conversion coatings on aluminum alloy 2024-T3 in a 100 mM NaCl solution. They found that vanadates were anodic and cathodic inhibitors in near-neutral solutions. Iannuzzi et al. [24,25] found that metavanadates inhibit AA2024-T3 corrosion by a mechanism that does not involve electrochemical reduction. However, decavanadates did not impart significant corrosion protection. Yang et al. [26] immersed magnesium alloy (AZ61) in vanadium containing bath with various conditions, such as the vanadium concentration, immersion time and bath temperature. The presented conversion treatment had its potential to replace the chrome-based conversion coating treatment.

In this work, a newly developed environmentally friendly vanadium conversion coating was proposed on the EG plates as alternatives to toxic chromate based systems. The effect of vanadium conversion coating on the corrosion behavior of EG plates in 3.5% NaCl solution will be studied using Tafel and EIS techniques. Surface examination will be performed by scanning electron microscopy (SEM) and X-ray photoelectron spectroscopy (XPS).

2. Experimental procedure

2.1. Materials and samples pre-treatments

Commercial electrogalvanized steel (EG) plates made by Baosteel Co. in China with coating mass on both sides of 60 g m^{-2} were employed as substrates. Before

* Corresponding author. Tel.: +86 451 86413721; fax: +86 451 86221048.
E-mail address: lininghit@yeah.net (N. Li).

0925-8388/$ – see front matter © 2010 Elsevier B.V. All rights reserved.
doi:10.1016/j.jallcom.2010.09.080

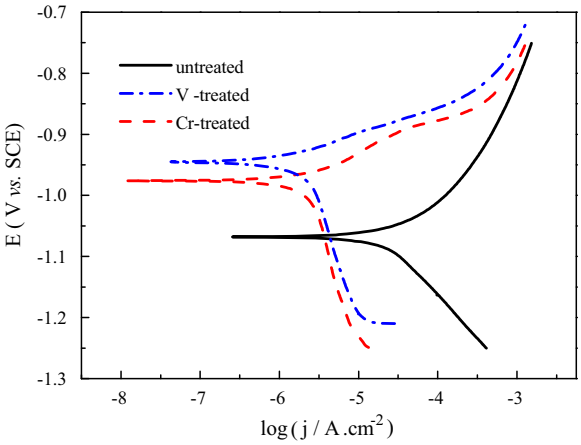

Fig. 1. Polarization curves of the EG plates for untreated, V-treated and Cr-treated EG plates tested in 3.5% NaCl solution at room temperature.

the vanadium conversion treatment, the specimen was degreased using ethanol and activated in a HNO_3 solution for 10 s, and then rinsed with deionised water. The vanadium conversion bath includes $NaVO_3$ (24 g/L), NaH_2PO_4 (8 g/L), and $K_3Fe(CN)_6$ (13 g/L). The pH of vanadium conversion bath was adjusted to 1.8 by adding H_3PO_4 into the bath with agitation. After activation process, the specimen was immersed in vanadium conversion bath at room temperature for 60 s, and then washed with distilled water to stop the future reaction via removing the residual salts. After drying in compressed air, the V-treated EG sample was obtained and stood for overnight to test.

For comparison, a chromate treatment is also used. The untreated EG plate was immersed in the solution containing 5 g/L CrO_3 and 2 g/L $ZnSO_4$ solution for 30 s at 20–25 °C and pH 1.5, then rinsed in distilled water and dried with compressed air.

2.2. Electrochemical techniques

The electrochemical properties of both as-received and conversion-treated samples were performed at room temperature by the potentio-dynamic electrochemical tests to evaluate the corrosion resistances. Tafel test with scan rate of 5 mV s^{-1} from −1.3 to −0.7 V (vs. OCP) started after the open circuit potential was stable. EIS curves were measured by immersion the samples (0.785 cm^2 of exposed area) into a 3.5% NaCl solution at pH 6.8 with an EG&G PAR273 potentiostat, applying 10 mV amplitude signals over a 10^4 to 10^{-2} Hz frequency range. This equipment comprised three electrodes, the sample is the working electrode, and platinum mesh is the counter electrode and the saturated calomel electrode (SCE) as the reference electrode.

2.3. Surface analysis

The surface morphologies of the samples were observed by scanning electron microscopy (Hitachi, S-4700). X-ray photoelectron spectroscopy (XPS) analyses were performed with a PHI5700 ESCA system (Perkin-Elmer) using Al Kα radiation (1486.6 eV), operated at a constant power of 250 W. The pressure in XPS analysis chamber was maintained below 10^{-7} Pa during the measuring period. The high-resolution spectra were taken with the pass energy of 29.35 eV and the step size of 0.125 eV. Charging compensation was undertaken by assuming that the O1s level at 284.5 eV for C1s. The analyzed surface area was around 4 mm × 4 mm. Quantification was done by calculating the elemental peak area which corrected according to the sensitivity factors after background subtraction. To obtain atomic concentration profiles (distribution of elements as a function of specimen thickness), the surface was sputtered by Ar^+ bombardment at a 3 kV and the sputtering rate was around 20 Å min^{-1}. The XPS data analysis was performed with XPSPeak4.1 program.

3. Results and discussion

3.1. Electrochemical results

Potentio-dynamic measurement was used to study corrosion behavior of the three EG plates in contact with a 3.5% NaCl solution at pH 6.8. Fig. 1 shows three typical polarization curves for the V-treated, untreated and Cr-treated EG plates tested in 3.5% NaCl solution. E_{corr} are −0.908 V for V-treated layer, −1.068 V for untreated EG plate, and −0.951 V for Cr-treated layer. Both cathodic reaction and anodic reaction of the two treated EG plates are inhibited markedly compared with the untreated EG plate, and the inhibition effectiveness of anodic reaction is higher than that of cathodic reaction. Comparing the left shift of the Tafel polarization for treated EG plates, it is found that the anodic branch for V-treated EG plate is approached to that for Cr-treated plate and far away from that for untreated EG plate. It can be considered that the suppression the anodic process of zinc corrosion by the vanadate coatings is chiefly dependent on the coverage of vanadate coatings.

Table 1
Corrosion data of the samples from Tafel tests.

Sample	E_{corr} (vs. SCE, V)	i_{corr} (A cm^{-2})
Untreated EG	−1.068	4.28×10^{-5}
Cr-treated EG	−0.951	2.39×10^{-6}
V-treated EG	−0.908	1.98×10^{-6}

Through Tafel extrapolation, corrosion potential (E_{corr}) and corrosion current density (i_{corr}) of three EG plates were obtained, which were listed in Table 1. The V-treated layer and Cr-treated layer increase corrosion potential of EG plate by 160 mV and 117 mV, respectively. And corrosion current density of the V-treated EG plate is 21 times lower than that of the untreated EG plate, and lower than that of the Cr-treated EG plate, indicating that both V-treatment and Cr-treatment seem to have a significant improvement on corrosion resistance of EG plate when exposed to the 3.5% NaCl solution and V-treatment provides better effectiveness. It suggested the corrosion protection provided by the V-treated layer is due to blocking of parts of the EG surface with reduction of oxygen and metal dissolution occurring in the pores of the coating layers.

3.2. EIS measurement

EIS measurement was also used to study corrosion behavior of the three EG plates in contact with a 3.5% NaCl solution. Fig. 2 presents three representative Nyquist plots for treated and untreated samples.

As Fig. 2(a) shows, the Nyquist plot of untreated sample presents a depressed semicircle, at high frequencies (HF), accompanied by a capacitive loop at low frequencies (LF), which resembles an inductive loop over the real axis. In chloride environment, the corrosion products such as zinc hydroxychlorides and zinc oxides are formed on the surface of zinc [27]. In the case of EDG, the HF capacitive loop can be ascribed to the formation of the corrosion products which suppress the process of charge transfer; the LF inductive loop can be attributed to the dissolution of the zinc layer [28–30]. The system has not been reached the steady state. It seems to the result of the reactivity of the aggressive electrolyte, for example chloride ion. The similar situation was mentioned in the literatures [31,32]. The equivalent circuit depicted in Fig. 3(a) was used in the simulation fitting procedure of EIS spectrum at high and intermediate frequencies. In the circuit, R_s corresponds to the resistance of the electrolyte; R_{ct} and CPE_{dl} represent the charge transfer resistance and the double layer capacitance, respectively.

As Fig. 2(b) and (c) shows, the shape of Nyquist plots is similar for Cr-treated and V-treated samples. The two Nyquist plots present a depressed semicircle at the higher frequencies, which can be attributed to charge transfer process of corrosion. The semicircle is followed, at the lower frequencies, by a straight line superimposed at 45° to both axes, which is corresponding to diffusion process. In this case, the two EIS spectra were fitted by the equivalent circuit of Fig. 3(b), where R_s corresponds to the resistance of the electrolyte, R_{ct} is the charge transfer resistance, CPE_{dl} is the double layer capacitance, and W represents the diffusion (Warburg) impedance.

The parameters used in the fitting procedure were presented in Table 2. As can be seen from Fig. 2, excellent agreement between experimental and simulated data is observed, and the fitting error

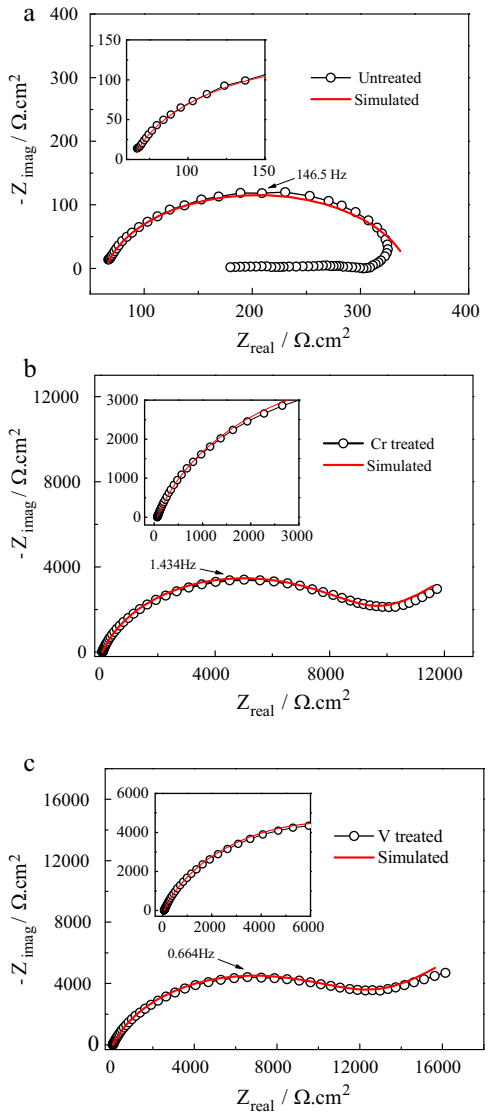

Fig. 2. Nyquist plots for the samples after 1 h of immersion in 3.5% NaCl solution at pH 6.8. (a) untreated EG plate; (b) Cr-treated EG plate; (c) V-treated EG plate.

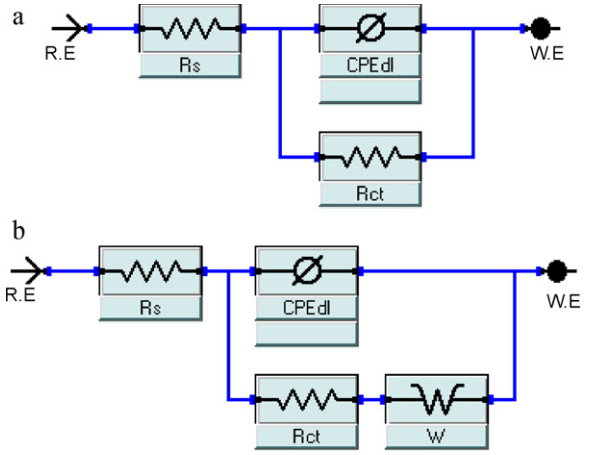

Fig. 3. Equivalent electrical circuit used to model: (a) untreated EG plate/3.5% NaCl solution system; and (b) Cr-treated and V-treated EG plates/3.5% NaCl solution system.

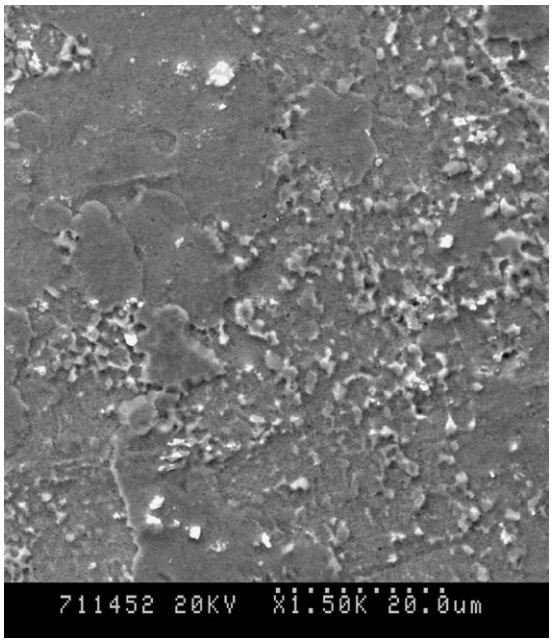

Fig. 4. SEM micrograph of the V-treated layer on EG plate.

here is less than 10%. Through fitting the impedance data, plenty of information is discovered. Charge transfer resistance (R_{ct}) of the two treated EG plates is remarkably higher than untreated EG plate and V-treated EG plate has the highest R_{ct}. The comparison indicates that V-treatment or Cr-treatment can remarkably improve corrosion resistance of EG plate in contact with 3.5% NaCl solution and V-treatment is more efficient, indicating that vanadium conversion coating has a high protection property, which may be the reason that V-treated EG plate has the highest R_{ct}.

3.3. Characterization of the V-treated layer

Fig. 4 shows a SEM micrograph of the V-treated layer on EG plate. From Fig. 4, it can be observed that V-treated layer is composed of the closely packed particles, and it is difficult to discern the boundary.

X-ray photoelectron spectroscopy (XPS) was used to analyze chemical composition of the vanadium conversion coating. Fig. 5

Table 2
Parameters used in the simulation of impedance data.

Element	Untreated EG plate		Cr-treated EG plate		V-treated EG plate	
	Values	Error (%)	Values	Error (%)	Values	Error (%)
R_s ($\Omega\,cm^2$)	64.54	1.29	63.05	0.49	66.36	0.39
Y_0 (CPE_{dl}) ($F\,s^{n-1}\,cm^{-2}$)	8.498E-6	7.79	1.856E-5	1.08	2.727E-5	0.94
n	0.877	1.17	0.802	0.25	0.777	0.20
R_{ct} ($\Omega\,cm^2$)	280.4	1.47	9087	0.98	11,960	0.66
Y_0 (W) ($F\,s^{-0.5}\,cm^{-2}$)	–	–	7.678E-4	3.43	5.877E-4	2.92

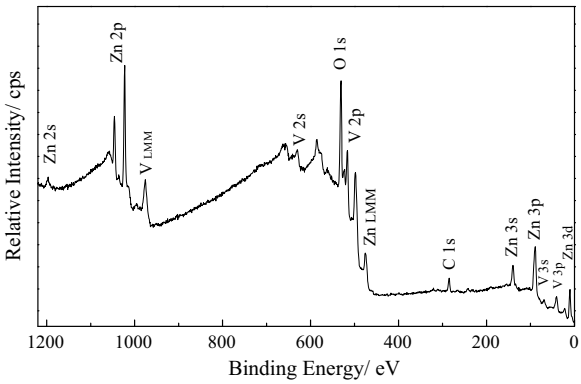

Fig. 5. XPS survey spectrum of the vanadium layer prepared on EG plate after 5 min of Ar^+ etching.

shows the whole XPS spectrum for the V-treated sample with 5 min Ar^+ etching. After Ar^+ etching, the signals of contaminants have become feeble. It can be seen from Fig. 5 that the photoelectron peak for V 2p appears clearly at a binding energy, E_b, of 524 eV, O 1s at E_b = 531 eV, Zn 2p at E_b = 1022 eV and C 1s at E_b = 285 eV. The chemical composition of the coating layer determined by integration of the peak area in the spectrum is V 21.77, O 56.71, Zn 17.71, C 3.81 (atom %). Obviously, the presence of carbon might be attributed to the residual carbon from precursor solution and the adventitious hydrocarbon from the XPS instrument itself.

Fig. 6 shows the high resolution XPS spectra of the Zn 2p, V 2p and O1s regions for the V-treated EG plate. The $Zn2p_{3/2}$ spectrum consists of one peak corresponding to zinc in form of Zn^{2+} at 1021.7 eV (Fig. 6(a)). The presence of zinc comes from the oxide film by the low pH of the coating bath. The binding energy of the $V\,2p_{1/2}$ and $V\,2p_{3/2}$ are found at 516.4 and 523.5 eV, respectively (Fig. 6(b)). After deconvolution with Gaussian functions, the V 2p region is decomposed into two contributions corresponding to the different oxidation states of vanadium. Each contribution consists of a doublet between the $2p_{3/2}$ and $2p_{1/2}$ peaks. The dominant doublet composed of two peaks located at 516.93 eV ($V2p_{3/2}$) and 524.44 eV ($V2p_{1/2}$) is assigned to V^{5+} [33–37]. The peaks of the minor doublet composed of two peaks located at 515.65 eV ($V2p_{3/2}$) and 523.91 eV ($V2p_{1/2}$), and assigned to V^{4+} [34–37].

Fig. 6(b) also shows the high resolution XPS spectra of the O 1s region for the vanadium conversion coating after 5 min Ar^+ etching. The O 1s region is composed of three peaks. The peak at 530.56 eV is attributed to V–O. The second one at 531.06 eV is attributed to OH^- existing as V–OH. The third one at 532.09 eV is attributed to adsorbed water and C–OH, C=O, C–O–C, and the last three ones are associated with the contaminants. In summary, it is believed that the vanadium coating mainly consists of vanadium and oxygen, which mainly exist as V^{5+}, V^{4+} and its hydrates.

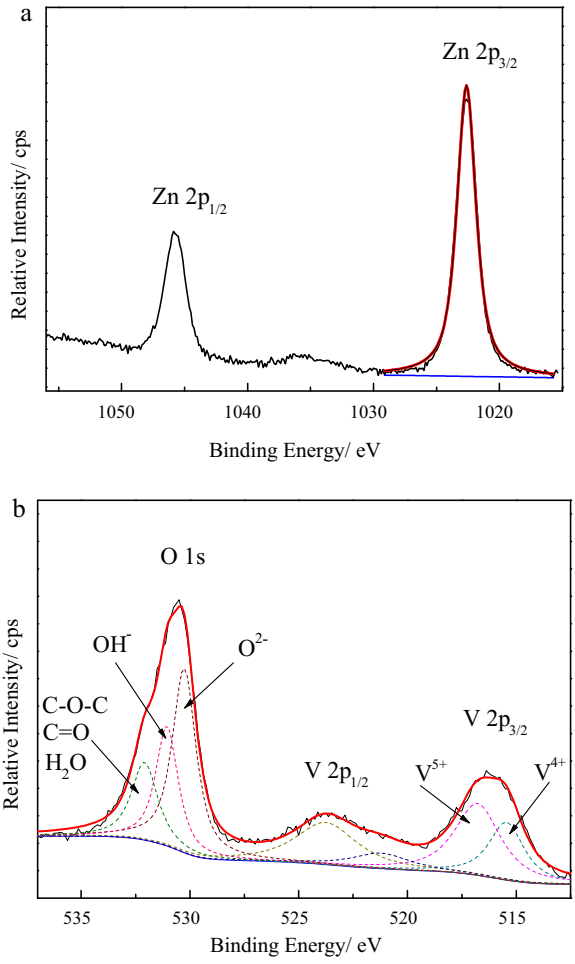

Fig. 6. High resolution XPS spectra of the Zn2p (a), V2p and O1s (b) for the V-treated EG plate.

4. Discussion

Vanadium conversion coating formation is essentially a sol–gel-like process. The formation of pentavalent vanadium oxides by condensation and polymerization has already been described quite thoroughly [38]. The ability to trigger the conversion coating formation depends on the interplay among the soluble vanadate ions, pH of the bath and changes in the solution pH at the metal–solution interface. The predominant species in solution is VO_2^+ when the pH is about 1.8, the species does not react to product condensed vanadium oxides [39]. When exposed to the EG plate surface with the coating bath, activation occurs due to surface catalyzed proton reduction such as dissolution of the oxide film by the low pH. For this reason, the interfacial pH increases and triggers formation of $VO(OH)_3$ by hydrolysis of VO_2^+.

$$VO_2^+ + 2H_2O \rightarrow VO(OH)_3 + H^+ \quad (1)$$

At pH values close to 2, coordination of $VO(OH)_3$ changes from tetrahedral to octahedral by a water addition reaction.

$$VO(OH)_3 + 2H_2O \rightarrow VO(OH)_3(OH_2)_2 \quad (2)$$

This hydrate then polymerizes by forming V(V)–V(V) linkages forming a so-called polymer backbone. In similar, V^{4+} gels may form by a hydrolysis–condensation–polymerization process analogous to those for V^{5+} gels. Simultaneously, vanadate binds via oxygen ligands forming V(V)–V(IV) linkages, which are characteristic of vanadium conversion coatings.

In this work, electrochemical polarization experiments demonstrated that the vanadium conversion coatings were able to protect EG plate against corrosion during exposure to 3.5% NaCl solution. The electrochemical results correlated well with the analytical data, EIS results showed that the uniform film hindered the initiation of the corrosion processes. On the other hand, polarization curves of the V-treated sample showed the marked suppression of anodic and cathodic processes and consequently improving corrosion resistance.

The above mechanism can be used to explain the improved corrosion resistance of EG plates pre-treated with vanadate solution during immersion in NaCl solutions. The protection mechanism seems to be closely associated with the presence of vanadium

oxides/hydroxides at the surface, hindering the corrosion processes.

5. Conclusions

The vanadium conversion coating as chromate replacement was prepared on EG plate by immersing in vanadate containing bath. According to potentio-dynamic measurement results, in 3.5% NaCl solution at pH 6.8, the V-treated EG plate presents the lowest i_{corr} (1.98×10^{-6} A cm^{-2}) as compared with the untreated EG plate (4.28×10^{-5} A cm^{-2}) and the Cr-treated EG plate (2.39×10^{-6} A cm^{-2}). Besides, the vanadium conversion coating significantly suppresses both the anodic reaction and cathodic reaction of EG plate corrosion, especially the anodic one. According to EIS results, the V-treated EG plate provides the highest R_{ct} (11,960 Ω cm^2) as compared with the untreated EG plate (280.4 Ω cm^2) and the Cr-treated EG plate (9087 Ω cm^2), indicating that Corrosion resistance of V-treated EG plate is much better than that of the untreated EG plate, and slightly better than that of Cr-treated EG plate. The vanadium conversion coating is composed of the closely packed particles. The coating mainly consists of vanadium and oxygen, which mainly exist V^{5+}, V^{4+} and its hydrates.

References

[1] F.W. Eppensteiner, M.R. Jennkind, Met. Finish. 105 (2007) 413–424.
[2] J.E. Gray, B. Luan, J. Alloys Compd. 336 (2002) 88–113.
[3] A.A.O. Magalhães, I.C.P. Margarit, O.R. Mattos, J. Electroanal. Chem. 572 (2004) 433–440.
[4] B.L. Lin, J.T. Lu, G. Kong, Corros. Sci. 50 (2008) 962–967.
[5] C.G. da Silva, I.C.P. Margarit-Mattos, O.R. Mattos, H. Perrot, B. Tribollet, V. Vivier, Corros. Sci. 51 (2009) 151–158.
[6] V. Mourtalier, M.P. Gigandet, L. Ricq, J. Pagetti, Appl. Surf. Sci. 183 (2001) 1–9.
[7] W. John, Bibber, Met. Finish. 106 (2008) 41–46.
[8] M. Hara, R. Ichino, M. Okido, N. Wada, Surf. Coat. Technol. 169–170 (2003) 679–681.
[9] R.P. Socha, Jan Fransaer, Thin Solid Films 488 (2005) 45–55.
[10] S. Dalbin, G. Maurin, R.P. Nogueira, Surf. Coat. Technol. 194 (2005) 363–371.
[11] R.P. Socha, Nicolas Pommier, Jan Fransaer, Surf. Coat. Technol. 201 (2007) 5960–5966.
[12] Y. Kangde, S. Shizhe, S. Ningxiang, Mater. Chem. Phys. 28 (1991) 303–308.
[13] G. Klimow, N. Fink, G. Grundmeier, Electrochim. Acta 53 (2007) 1290–1299.
[14] L. Zhu, F. Yang, N. Ding, Surf. Coat. Technol. 201 (2007) 7829–7834.
[15] M. Hosseini, H. Ashassi-Sorkhabi, H. Allah, Y. Ghiasvand, J. Rare Earth 25 (2007) 537–543.
[16] M.A. Arenas, C. Casado, V. Nobel-Pujol, J. de Damborenea, Cement Concrete Comp. 28 (2006) 267–275.
[17] B.R.W. Hinton, J. Alloys Compd. 180 (1992) 15–25.
[18] S. Bernal, F.J. Botana, J.J. Calvino, M. Marcos, J.A. Pérez-Omil, H. Vidal, J. Alloys Compd. 225 (1995) 638–641.
[19] R.E. Van de Leest, G. Krijl, Thin Solid Films 72 (1980) 237–246.
[20] C.G. da Silva, A.N. Correia, P. de Lima-Neto, I.C.P. Margarit, O.R. Mattos, Corros. Sci. 47 (2005) 709–722.
[21] A.S. Hamdy, D.P. Butt, J. Mater. Process. Technol. 181 (2007) 76–80.
[22] A.S. Hamdy, A.M. Beccaria, Corros. Prevent. Control 48 (2001) 143–149.
[23] H. Guan, R.G. Buchheit, Corrosion (Houston) 60 (2004) 284–296.
[24] M. Iannuzzi, J. Kovac, G.S. Frankel, Electrochim. Acta 52 (2007) 4032–4042.
[25] M. Iannuzzi, G.S. Frankel, Corros. Sci. 49 (2007) 2371–2391.
[26] K.H. Yang, M.D. Ger, W.H. Hwu, Y. Sung, Y.C. Liu, Mater. Chem. Phys. 101 (2007) 480–485.
[27] A. Amirudin, D. Thierry, Prog. Org. Coat. 28 (1996) 59–75.
[28] S. Jegannathan, T.S.N.S. Narayanan, K. Ravichandran, S. Rajeswari, Electrochim. Acta 51 (2005) 247–256.
[29] C. Cachet, F. Ganne, S. Joiret, G. Maurin, J. Petitjean, V. Vivier, R. Wiart, Electrochim. Acta 47 (2002) 3409–3422.
[30] B.L. Lin, J.T. Lu, G. Kong, Surf. Coat. Technol. 202 (2008) 1831–1838.
[31] M.A. Arenas, J. de Damborenea, Corros. Sci. 48 (2006) 3196–3207.
[32] C. Cacher, R. Wiart, J. Electroanal. Chem. 126 (1981) 103–114.
[33] Q.H. Wu, A. Thissen, W. Jaegermann, M. Liu, Appl. Surf. Sci. 236 (2004) 473–478.
[34] G. Silversmit, D. Depla, H. Poelman, G.B. Marin, R.D. Gryse, J. Electron. Spectrosc. Relat. Phenom. 135 (2004) 167–175.
[35] J. Mendialdua, R. Casanova, Y. Barbaux, J. Electron. Spectrosc. Relat. Phenom. 71 (1995) 249–261.
[36] G.A. Sawatzky, D. Post, Phys. Rev. B 20 (1979) 1546–1555.
[37] M. Demeter, M. Neumann, W. Reichelt, Surf. Sci. 454–456 (2000) 41–44.
[38] J. Livage, Solid State Ionics 86–88 (1996) 935–942.
[39] M. Henry, J.P. Jolivet, J. Livage, Struct. Bond. 77 (1992) 153–206.